Fiber core mode leakage induced by refractive index variation in high-power fiber laser*

Ping Yan(闫平), Xuejiao Wang(王雪娇), Yusheng Huang(黄昱升), Chen Fu(付晨), Junyi Sun(孙骏逸), Qirong Xiao(肖起榕), Dan Li(李丹)†, and Mali Gong(巩马理)

Center for Photonics and Electronics, Department of Precision Instruments, Tsinghua University, Beijing 100084, *China*

(Received 19 September 2016; revised manuscript received 17 November 2016; published online 23 January 2017)

This paper presents an investigation of specific optical fiber core mode leakage behavior that occurs in high-power double-clad fiber lasers as a result of thermally-induced refractive index variations. A model of the power transfer between the core modes and the cladding modes during thermally-induced refractive index variations is established based on the mode coupling theory. The results of numerical simulations based on actual laser parameters are presented. Experimental measurements were also carried out, the results showed good agreement with the corresponding simulation results.

Keywords: double-clad fiber laser and amplifier, core loss, cladding mode, mode coupling theory

PACS: 42.55.Wd, 42.60.Da, 42.55.Xi **DOI:** 10.1088/1674-1056/26/3/034205

1. Introduction

High-power fiber lasers have undergone unprecedented development over the last decade[1] and have evolved from watt-level laboratory curiosities into multi-kilowatt-scale systems with high market penetration. Their outstanding characteristics, which include high power scalability and stability, high optical efficiency, excellent beam quality, small footprint, and low weight, have become the trademarks of fiber lasers.

To operate under continuous wave multi-kilowatt power or pulsed high peak power conditions, the optical fibers used in these lasers require a large mode field diameter (MFD) to reduce the impact of nonlinear effects such as stimulated Raman scattering[2,3] and self-phase modulation on the laser performance. However, it is extremely challenging to increase the MFD while maintaining the outstanding beam quality characteristics of the fiber laser. To reduce the capacity of the transverse mode and thus ensure that fiber lasers operate under single-mode conditions or with only a few low-order modes, the refractive index difference between the fiber core and the fiber cladding must be strictly controlled.

Under the weakly guiding approximation, the refractive index changes in the fiber core or the fiber inner cladding cause variations in both the transverse mode capacity and the mode stability. As a result, the guided modes in the core region can leak into the cladding region and propagate with a larger numerical aperture. This irreversible process will lead to deterioration of the laser's efficiency, power density, and beam quality.

Refractive index variations can be induced by various factors, including excessive fiber bending[4] and splice misalignment;[5] however, these factors are not significantly related to the laser power level. This paper discusses the process of core mode coupling into the cladding and the subsequent propagation of these modes as cladding modes as a result of thermal effects in high-power fiber lasers. Based on the analysis presented here, the relationship between the fiber core leakage loss and the fiber laser's characteristics (e.g., cooling conditions, beam quality) is described.

In an initial effort to understand this process, the analysis focused on thermally-induced refractive index variations in the fiber core region of high-power fiber lasers. Additionally, the coupling coefficients of several typical low-order linear polarization modes coupled to the cladding modes in double-clad fibers were derived. The physical origins of the mode coupling loss in fiber lasers were discussed and a model of these losses was proposed, before the proportion of leaky modes in fiber lasers and amplifiers was numerically simulated using actual laser parameters. Experimental measurements subsequently provided data that verified these simulation results.

2. Thermally-induced refractive index variation in fiber lasers

A schematic illustration of the proposed fiber amplifier model is shown in Fig. 1. Heat is generated in the optical fiber by absorption of the pumping power, which results in changes in the refractive index. Before the analysis can be performed, the power distributions of the core modes in a typical fiber laser amplifier must be calculated. The rate equations that consider the distributions of the transverse and longitudinal gains and the mode fields in a cylindrical coordinate system can be expressed in the form of the following equation set:[6]

*Project supported by the National Natural Science Foundation of China (Grant Nos. 61307057 and 61675114).

†Corresponding author. E-mail: dli@mail.tsinghua.edu.cn

© 2017 Chinese Physical Society and IOP Publishing Ltd

$$\frac{N_2(r,\theta,z)}{N_1(r,\theta,z)} = \frac{\dfrac{[P_{\rm p}^+(z)+P_{\rm p}^-(z)]\sigma_{\rm ap}\varphi_{\rm p}(r,\theta)}{h\nu_{\rm p}} + \sum_{i=1}^{M_{\rm s}} \dfrac{[P_{si}^+(z)+P_{si}^-(z)]\sigma_{\rm as}\varphi_{si}(r,\theta)}{h\nu_{\rm s}}}{\dfrac{[P_{\rm p}^+(z)+P_{\rm p}^-(z)]\sigma_{\rm ep}\varphi_{\rm p}(r,\theta)}{h\nu_{\rm p}} + \dfrac{1}{\tau} + \sum_{i=1}^{M_{\rm s}} \dfrac{[P_{si}^+(z)+P_{si}^-(z)]\sigma_{\rm es}\varphi_{si}(r,\theta)}{h\nu_{\rm s}}},$$

$$\pm\frac{{\rm d}P_{\rm p}^{\pm}(z)}{{\rm d}z} = \left\{\int_0^{2\pi}\int_0^a \left[\sigma_{\rm ep}N_2(r,\theta,z) - \sigma_{\rm ap}N_1(r,\theta,z)\right]\varphi_{\rm p}(r,\theta)r{\rm d}r{\rm d}\theta\right\}P_{\rm p}^{\pm}(z) - \alpha_{\rm p}P_{\rm p}^{\pm}(z),$$

$$\pm\frac{{\rm d}P_{si}^{\pm}(z)}{{\rm d}z} = \left\{\int_0^{2\pi}\int_0^a \left[\sigma_{\rm es}N_2(r,\theta,z) - \sigma_{\rm as}N_1(r,\theta,z)\right]\varphi_{si}(r,\theta)r{\rm d}r{\rm d}\theta\right\}P_{si}^{\pm}(z)$$
$$- \alpha_{si}P_{si}^{\pm}(z) + 2\sigma_{\rm es}N_2(r,\theta,z)\cdot\frac{hc^2}{\lambda_{\rm s}^3}\Delta\lambda_{\rm s} + \sum_j {\rm d}_{ij}[P_{si}^{\pm}(z) - P_{sj}^{\pm}(z)]. \quad (1)$$

Here, the amplified spontaneous emission (ASE) spectrum is divided into $M_{\rm s}$ channels and each channel is marked using the subscript i (where $i = 1,2,\ldots,M_{\rm s}$). $N_2(r,\theta,z)$ and $N_1(r,\theta,z)$ represent the population densities of the upper and lower levels, respectively. $P_{\rm p}^+(z)$ and $P_{\rm p}^-(z)$ are the pump powers in the forward and backward directions, respectively, and $P_{si}^+(z)$ and $P_{si}^-(z)$ are the signal laser powers of the i-th channel in the forward and backward directions, respectively. $\sigma_{\rm ap}$ ($\sigma_{\rm ep}$) and $\sigma_{\rm as}$ ($\sigma_{\rm es}$) are the absorption (emission) cross-sections of the pump light and the laser, respectively. $\sigma_{\rm ap}$ and $\sigma_{\rm ep}$ are 2.34×10^{-24} m ^{2} and 2.34×10^{-24} m^2, respectively. $\sigma_{\rm as}$ and $\sigma_{\rm es}$ of the laser are 6.58×10^{-27} m^2 and 3.11×10^{-25} m^2, respectively. The loss factor of the pump light, $\alpha_{\rm p}$, and the loss factor of the laser, α_{si}, are 2.0×10^{-3} m^{-1} and 4.0×10^{-4} m^{-1}, respectively. $\Delta\lambda_{\rm s}$ is the spectral width of the signal laser and $2\sigma_{\rm es}N_2(r,\theta,z)\cdot\frac{hc^2}{\lambda_{\rm s}^3}\Delta\lambda_{\rm s}$ describes the influence of ASE on the mode power. When the seed power is strong enough, the ASE can be neglected and $2\sigma_{\rm es}N_2(r,\theta,z)\cdot\frac{hc^2}{\lambda_{\rm s}^3}\Delta\lambda_{\rm s}$ can be set as 0.[7] $\varphi_{\rm p}(r,\theta)$ and $\varphi_{si}(r,\theta)$ are the power normalized intensity distributions of the pump laser and the i-th laser mode, respectively. The boundary conditions for the power normalized intensity distribution of the pump laser and the i-th laser mode are set as

$$\int_0^{2\pi}\int_0^{\infty}\varphi_{si}(r,\theta)r{\rm d}r{\rm d}\theta = 1,$$
$$\int_0^{2\pi}\int_0^{\infty}\varphi_{\rm p}(r,\theta)r{\rm d}r{\rm d}\theta = 1. \quad (2)$$

In these equations, the pump light is considered even distributed and contains numerous high order modes. Therefore, the normalized pump light intensity can be expressed by the area of the inner-cladding $A_{\rm clad}$ as $\varphi_{\rm p}(r,\theta) = 1/A_{\rm clad}$. The d_{ij} denotes the power coupling coefficient of the i-th mode and the j-th mode.

To compare the theoretical figures with the experimental results, the actual parameters of the fiber amplifier are used to construct the simulation models, and these parameters are listed in Table 1. The power coupling coefficient is neglected by setting $d_{ij} = 0$ during the simulation. The simulation results are shown in Fig. 2, and indicate that a total laser output power of 666 W at 1080 nm is obtained, with 347 W in the LP_{01} mode and 319 W in the LP_{11} mode under launched pump power conditions of 750 W@975 nm. The beam quality is given as $M_x^2 = 1.54$ and $M_y^2 = 1.95$.

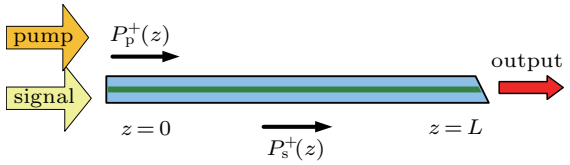


Fig. 1. (color online) Schematic illustration of the fiber amplifier model.

Table 1. Parameters used for fiber amplifier.

Parameters	Values
Pump power	750 W
Pump length	975 nm
Signal length	1080 nm
Gain fiber diameter	20/400 μm
NA	0.06/0.46
Absorption coefficient at 975 nm	1.26 dB/m
Length of gain fiber	25 m
Seed power	30 W

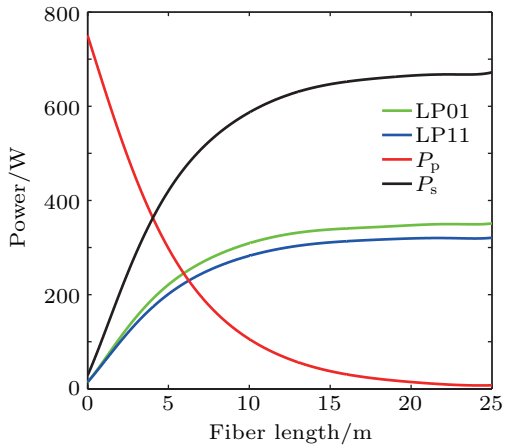


Fig. 2. (color online) Simulation results for the fiber amplifier rate equation when mode competition theory is considered.

When the pump power is absorbed, it generates heat in the fiber. The geometry of the fiber structure is shown in Fig. 3. The radial coordinate is r and the tangential angle is φ. The symbols a, b, and c represent the core, inner cladding, and

coating radii, respectively. To determine the radially varying refractive index that results from $\mathrm{d}n/\mathrm{d}T$, it is necessary to calculate the temperature distribution in the fiber.

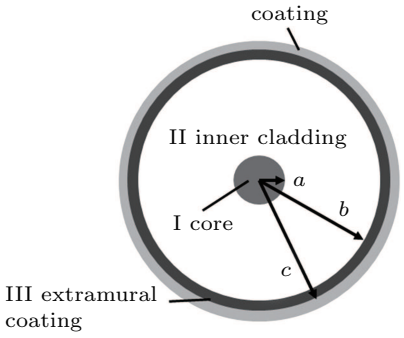


Fig. 3. Diagram showing cross-section of the fiber.

To calculate the temperature profile $T(r,\varphi,z)$ inside the optical fiber, the following equation is applied using azimuthal φ variations while the longitudinal thermal conduction is ignored:

$$\frac{1}{r}\frac{\partial}{\partial r}\left(r\frac{\partial T(r,z)}{\partial r}\right)=-\frac{Q(z)}{k}, \tag{3}$$

where r is the radial coordinate and z is the longitudinal coordinate along the fiber axis. $Q(z)$ is the thermal load power per unit volume in the fiber laser and k is the thermal conductivity of silica. The equation assumes that the heat power $Q(z)$ is uniform throughout the fiber core and can be acquired from the following expression:[8]

$$Q(z)=\left(1-\frac{\lambda_{\mathrm{p}}}{\lambda_{\mathrm{l}}}\right)\frac{P_{\mathrm{abs}}(z)}{\Delta V}, \tag{4}$$

where $P_{\mathrm{abs}}(z)$ is the absorbed pump power in a differential fiber element of volume. Subject to the aforementioned boundary conditions, which are expressed in Eq. (4), the equations are then transformed into the subsequent expressions for the temperatures in regions I, II, and III:

$$\begin{aligned}
&\frac{\partial T(0)}{\partial r}=0,\quad T(0)=T_0,\\
&\frac{\partial T_{\mathrm{I}}(a)}{\partial r}=\frac{\partial T_{\mathrm{II}}(a)}{\partial r},\quad T_{\mathrm{I}}(a)=T_{\mathrm{II}}(a),\\
&\frac{\partial T_{\mathrm{II}}(b)}{\partial r}=\frac{\partial T_{\mathrm{III}}(b)}{\partial r},\quad T_{\mathrm{II}}(b)=T_{\mathrm{III}}(b),\\
&\frac{\partial T_{\mathrm{III}}(c)}{\partial r}=\frac{h}{k_3}[T_{\mathrm{c}}-T_{\mathrm{III}}(c)],\\
&T_{\mathrm{III}}(r,z)=T_{\mathrm{s}}+\frac{a^2\times Q(z)}{2k_2}\times\ln\left(\frac{c}{r}\right),\quad (b\le r\le c),\\
&T_{\mathrm{II}}(r,z)=T_{\mathrm{III}}(b,z)+\frac{a^2\times Q(z)}{2k_1}\times\ln\left(\frac{b}{r}\right),\quad (a\le r\le b),\\
&T_{\mathrm{I}}(r,z)=T_{\mathrm{II}}(a,z)+\frac{Q(z)}{4k_1}(a^2-r^2),\quad (0\le r\le a),\\
&Q(z)\mathrm{d}V=\mathrm{d}S\times h(T_{\mathrm{s}}-T_{\mathrm{c}}),
\end{aligned} \tag{5}$$

$$\tag{6}$$

where k_1, k_2, and k_3 are the thermal conductivities of silica, the cladding, and the coating material, respectively, T_{s} is the fiber surface temperature, and T_{c} is the coolant temperature. h represents the convective coefficient. Based on the fiber temperature field $T(r,\ z)$ and the temperature coefficient of the refractive index $\beta_1=(\mathrm{d}n/\mathrm{d}T)$, the resulting refractive index variation field $\Delta n(r,z)$ can be calculated as

$$\Delta n(r,z)=\beta_1[T(r,z)-T_{\mathrm{c}}]. \tag{7}$$

It should be noted here that the temperature difference between the boundary and the center of the core is small when the pump power is launched at sub-kilowatt levels. For example, when a pump power of 1000 W is launched, the temperature difference is calculated to be 7.06 °C. The corresponding refractive index variation is approximately 8.33×10^{-5}, and can thus be neglected. Therefore, the refractive index variation can be considered to have the same value over the entire fiber core area. Based on the simulation results for the fiber amplifier rate equation and Eqs. (4)–(6), the calculated thermally-induced fiber core refractive index variations along the fiber length are as shown in Fig. 4. Here, the refractive index variation is caused by the thermal effects of the fiber amplifier at multi-kilowatt power levels. According to the mode coupling theory, these variations will cause a mode coupling process between the core modes and the cladding modes and the corresponding power transfer and fiber core losses, which will be discussed in subsequent sections.

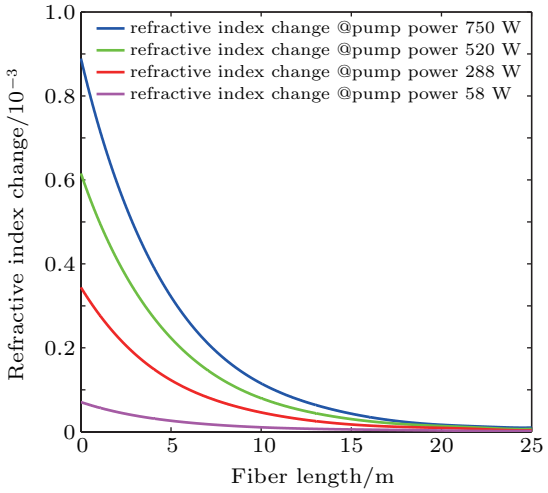


Fig. 4. (color online) Fiber thermal conditions and thermally-induced fiber core refractive index variations.

3. Mode coupling coefficient between core modes and cladding modes

As described in Section 2, a thermally-induced change in the refractive index occurs when the pump power is absorbed in the fiber, and this leads to the mode coupling process. This paper describes the coupling process between a guided core

mode and the cladding modes in a typical step-index fiber in detail. The interactions between the fiber mode order υ and the refractive index variation μ in a step-index fiber can be described using the coupling coefficients, which are defined as follows:[9–11]

$$\kappa_{\nu\mu}(z) = \frac{\omega}{4}\int_0^{2\pi} \mathrm{d}\phi \int_0^{\infty} r\mathrm{d}r\Delta\varepsilon(r,\phi,z)\times E_{\nu}(r,\phi)E_{\mu}^{*}(r,\phi). \quad (8)$$

Here, E_{ν} and E_{μ} are the transverse components of the mode electric fields that are labeled ν and μ (further details can be found in Ref. [8]). It should be noted here that the core mode field is much weaker in the cladding region than that in the core region, while the refractive index variation in the core region is several times higher than that in the cladding region. Therefore, the discussion in this paper focuses solely on the coupling process in the fiber core region.

In the weakly guiding approximation, the transverse field components of the core modes in the core region (where $r \le a$) can be expressed under linear polarization conditions as[12]

$$E_{lm,r}^{\mathrm{co}} = \mathrm{i}E_{lm}^{\mathrm{co}}\mathrm{J}_1(u_{lm}r)\begin{Bmatrix}\cos l\phi\\ \sin l\phi\end{Bmatrix}\exp[\mathrm{i}\phi]\exp[\mathrm{i}(\beta_2 z-\omega t)],$$
$$E_{lm,\phi}^{\mathrm{co}} = -E_{lm}^{\mathrm{co}}\mathrm{J}_1(u_{lm}r)\begin{Bmatrix}\cos l\phi\\ \sin l\phi\end{Bmatrix}\exp[\mathrm{i}\phi]\exp[\mathrm{i}(\beta_2 z-\omega t)], \quad (9)$$

where $\mathrm{J}_1(u_{lm}r)$ is the Bessel function of the first kind, $\beta_2 = (2\pi/\lambda)\,n_{\mathrm{eff}\,lm}$ is the propagation constant, and E_{lm}^{co} is a normalization coefficient. The transverse electric field components of the cladding modes of azimuthal order l in the core region (where $r \le a$) can be expressed as[9,12]

$$\begin{aligned}E_{lm,r}^{\mathrm{cl}} &= \mathrm{i}E_{lm}^{\mathrm{cl}}\frac{u_{lm}}{2}\times\exp(\mathrm{i}l\phi)\exp[i(\beta_2 z-\omega t)]\\ &\quad\times\Big\{\mathrm{J}_{l+1}(u_{lm}r)+\mathrm{J}_{l-1}(u_{lm}r)\\ &\quad-\frac{\sigma\zeta_0}{ln_1^2}[\mathrm{J}_{l+1}(u_{lm}r)-\mathrm{J}_{l-1}(u_{lm}r)]\Big\},\\ E_{lm,\phi}^{\mathrm{cl}} &= E_{lm}^{\mathrm{cl}}\frac{u_{lm}}{2}\times\exp(\mathrm{i}l\phi)\exp[i(\beta_2 z-\omega t)]\\ &\quad\times\Big\{\mathrm{J}_{l+1}(u_{lm}r)-\mathrm{J}_{l-1}(u_{lm}r)\\ &\quad-\frac{\sigma\zeta_0}{ln_1^2}[\mathrm{J}_{l+1}(u_{lm}r)+\mathrm{J}_{l-1}(u_{lm}r)]\Big\},\end{aligned} \quad (10)$$

where $\sigma = \mathrm{i}ln_{\mathrm{eff}\,lm}Z_0$. Here, l is the azimuthal mode number, E_{lm}^{cl} is the field normalization constant, and ζ_0 is a parameter related to the dispersion of the cladding modes of azimuthal number l.[9,12] This definition is discussed in greater detail in Ref. [8]. It should be noted that if all cladding modes (with any l) are included in Eqs. (7)–(9), then the azimuthal integral becomes

$$\int_o^{2\pi} R(\phi)\times\exp(\mathrm{i}(1-l_{\mathrm{cl}})\phi),$$
$$R(\phi) = \begin{cases}\cos l_{\mathrm{co}}\phi, & \text{even core modes},\\ \sin l_{\mathrm{co}}\phi, & \text{odd core modes},\end{cases} \quad (11)$$

where l_{cl} is the number of cladding modes. For the LP_{01} mode, the only nonzero coupling constants are those between the LP_{01} core mode and the cladding modes where $l_{\mathrm{cl}} = 1$.[9,12] For the LP_{11} mode, the phase expressions are expanded, and the azimuthal integral can then be expressed as

$$\int_o^{2\pi}\cos(\phi)\cos((l_{\mathrm{cl}}-1)\phi)+\mathrm{i}\cos(\phi)\sin((l_{\mathrm{cl}}-1)\phi) = \pi\delta_{\mathrm{cl}-1},$$
even mode,
$$\int_o^{2\pi}\sin(\phi)\cos((l_{\mathrm{cl}}-1)\phi)+\mathrm{i}\sin(\phi)\sin((l_{\mathrm{cl}}-1)\phi) = \mathrm{i}\pi\delta_{\mathrm{cl}-1},$$
odd mode. (12)

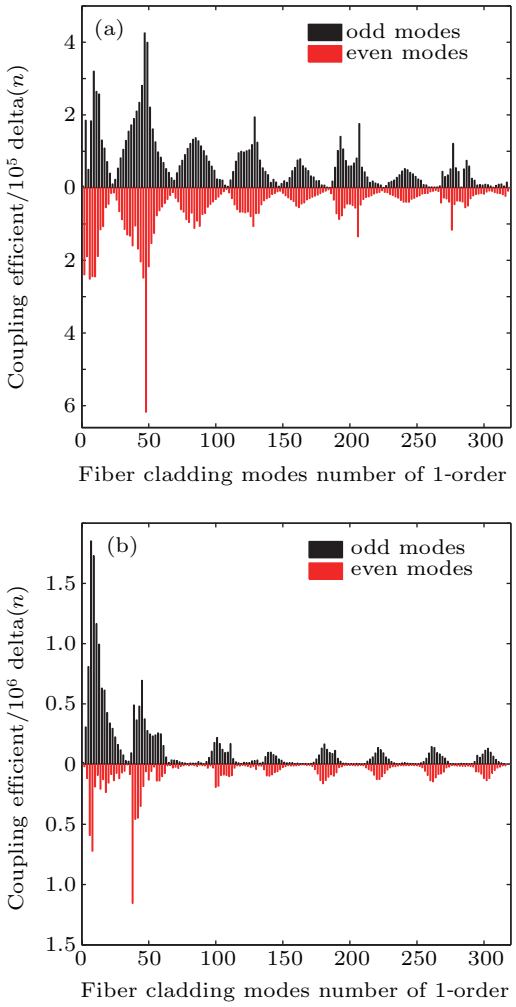


Fig. 5. (color online) (a) Mode coupling coefficient of LP_{01} core mode to the first-order cladding modes; (b) mode coupling coefficient of LP_{11} core mode to the second-order cladding modes.

In the above equations, $\delta_{\mathrm{cl}-1}$ is equal to 1 when $l_{\mathrm{cl}} = 2$, and is equal to 0 when $l_{\mathrm{cl}} \neq 2$. Therefore, the only nonzero coupling constants are those between the LP_{11} mode and the second-order cladding modes. The mode coupling coefficients of the LP_{11} even mode and the LP_{11} odd mode are a real number and an imaginary number, respectively. This means that the cladding mode sub-wave that is produced by the LP_{11} even mode has a 90° phase difference with that produced by the

LP_{11} odd mode at the same position in the fiber laser. Simulations were performed to calculate the coupling coefficients of the LP_{01} mode to the first-order cladding modes and the LP_{11} mode to the second-order cladding modes, the results are shown in Fig. 5.

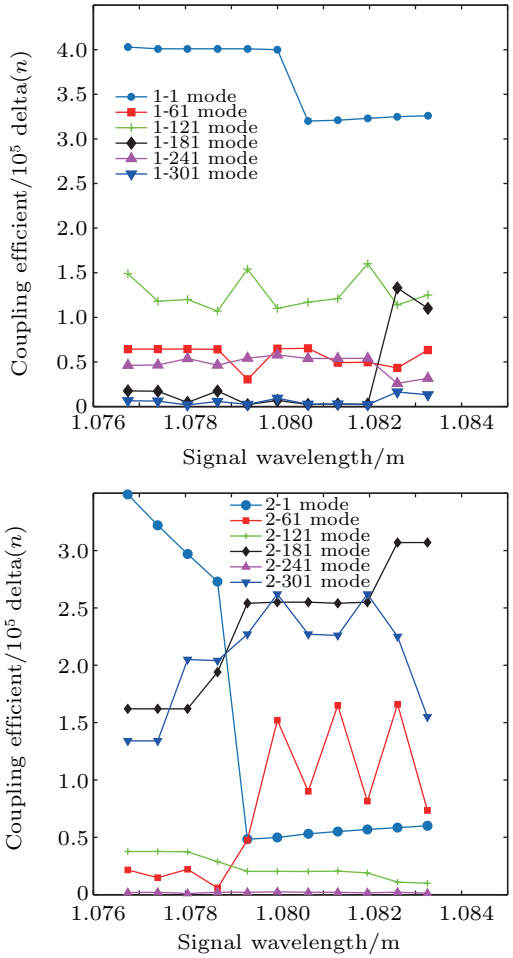


Fig. 6. (color online) (a) Variation of LP_{01} core mode coupling coefficient to specifically numbered cladding modes with the wavelength; (b) variation of LP_{11} core mode coupling coefficient to specifically numbered cladding modes with the wavelength.

Figure 5 shows that the coupling coefficients of the LP_{01} mode and the LP_{11} mode when coupling into the even cladding mode are larger than the corresponding coefficients when coupling into the neighboring odd mode. The coupling coefficient of the LP_{11} mode into the cladding modes is much higher than that of the LP_{01} mode. In Fig. 5(b), the coupling process of the LP_{11} mode into the low numbers of the second-order cladding modes is shown to be very strong; the main part of the core leakage losses is taken up into the cladding modes, and this will be discussed in Section 4. To avoid the interference phenomenon of different cladding modes coupling to the same wave, the simulation process must also consider the spectral width of the fiber laser used in our experiments. Figure 6 shows the relationship between the variations in the coupling coefficients of the LP_{01} mode and the LP_{11} mode to a specific cladding mode and the signal laser wavelength over the range from 1077 nm to 1083 nm when our experiment was performed at 1080 nm with a 3 dB bandwidth of approximately 1 nm.

4. Mode coupling and core mode loss process in fiber amplifier

Because the mode coupling coefficients have been obtained, the field amplitude can then be calculated using Eq. (13). The increment in the cladding mode's lv amplitude (where l is the cladding mode order and v is the cladding mode number) is expressed on the basis of the general coupled-mode equations that describe the variations in the forward- and backward-propagating amplitudes of a mode that result from the presence of other modes near a dielectric variation in the fiber[9,11]

$$\frac{\mathrm{d}A_{lv}}{\mathrm{d}z} = \mathrm{i}\sum_{\mu} A_{\mu} K_{u-lv} \exp[\mathrm{i}(\beta_u - \beta_{lv})z] + \mathrm{i}\sum_{\mu} B_{\mu} K_{u-lv} \exp[-\mathrm{i}(\beta_u + \beta_{lv})z], \tag{13}$$

where A_{lv} is the amplitude of the forward cladding mode lv, A_{μ} is the amplitude of the forward core mode u, B_{μ} is the amplitude of the backward core mode u, $\beta = (2\pi/\lambda)n_{\mathrm{eff}}$ is the propagation constant, and K_{u-1v} is the coupling coefficient between u and lv. Based on Eq. (13), we combine mode coupling, including fiber core mode coupling and clad mode coupling, with the rate equations. With further refinement, the new rate equations contain amplitude factors of core modes and clad modes as follows:

$$\begin{aligned}
\pm\frac{\mathrm{d}A_{si}^{\pm}(z)}{\mathrm{d}z} &= \sqrt{\left\{\int_0^{2\pi}\int_0^{a}\left[\sigma_{\mathrm{es}}N_2(r,\theta,z) - \sigma_{\mathrm{as}}N_1(r,\theta,z)\right]\varphi_{si}(r,\theta)\,r\,\mathrm{d}r\,\mathrm{d}\theta\right\}}A_{si}^{\pm}(z) - \alpha_{\mathrm{asi}}A_{si}^{\pm}(z) + \sqrt{2\sigma_{\mathrm{es}}N_{\mathrm{w}}(r,\theta,z)\cdot\frac{hc^2}{\lambda_{\mathrm{s}}^3}\Delta\lambda_{\mathrm{s}}}\cdot A_{si}^{\pm}(z) \\
&\quad + \mathrm{i}\sum_j A_{\mathrm{c}j}^{\pm}(z)\,K_{\mathrm{c}j-i}^{\mathrm{t}}(z)\exp\left[\mathrm{i}\left(\beta_i - \beta_{\mathrm{c}_j}\right)z\right] - \mathrm{i}\sum_k A_{si}^{\pm}(z)\,K_{\mathrm{c}_k}^{\mathrm{t}}(z)\exp\left[\mathrm{i}\left(\beta_{\mathrm{c}_k} - \beta_i\right)z\right], \\
\pm\frac{\mathrm{d}A_{\mathrm{c}j}^{\pm}(z)}{\mathrm{d}z} &= \mathrm{i}\sum_i A_{si}^{\pm}(z)\,K_{i-c_j}(z)^{\mathrm{t}}\exp\left[\mathrm{i}\left(\beta_i - \beta_{\mathrm{c}_j}\right)z\right],
\end{aligned} \tag{14}$$

where $P_{si}^{+}(z)$ and $P_{si}^{-}(z)$ are the power of the i-th fiber mode. Their corresponding complex amplitudes are $A_{si}^{+}(z)$ and $A_{si}^{-}(z)$, respectively, where $P_{si}(z) = |A_{si}(z)|^2$. $A_{\mathrm{c}_k}^{+}(z)$ and $A_{\mathrm{c}_k}^{-}(z)$ are the complex amplitudes of the k-th clad modes propagating in the

forward and backward directions, respectively. $K_{ij}(z)^{\mathrm{t}}$ is the transverse coupling coefficient for modes from i-th to j-th at position z. The factor

$$\sqrt{\left\{\int_0^{2\pi}\int_0^{a}\left[\sigma_{\mathrm{es}}N_2(r,\theta,z)-\sigma_{\mathrm{as}}N_1(r,\theta,z)\right]\varphi_{si}(r,\theta)\,r\,\mathrm{d}r\,\mathrm{d}\theta\right\}}A_{si}^{\pm}(z)$$

stands for the excess fiber core power induced by the gain. The factors $+\mathrm{i}\sum_j A_{si}^{\pm}(z)K_{ji}^{\mathrm{t}}(z)\exp\left[\mathrm{i}\left(\beta_j-\beta_i\right)z\right]$ and $-\mathrm{i}\sum_k A_{si}^{\pm}(z)K_{i-\mathrm{c}_k}^{\mathrm{t}}(z)\exp\left[\mathrm{i}\left(\beta_{\mathrm{c}_k}-\beta_i\right)z\right]$ represent the increased or reduced amplitude of the fiber core induced by the coupling among the fiber modes and clad modes. And $A_{\mathrm{c}j}^{\pm}(z)$ is the gain induced by mode coupling.

The amplitude attenuation of the core modes and the gain of the cladding modes caused by mode coupling along the fiber axis induced by the refractive index variations is calculated. Then, the intensity of the cladding modes at the fiber's output end is acquired. Figure 7 shows the gains of the first-order and the second-order cladding modes at the output end of the fiber laser used in this study. Importantly, this cladding mode power indicates the leakage losses of the LP_{01} and LP_{11} modes.

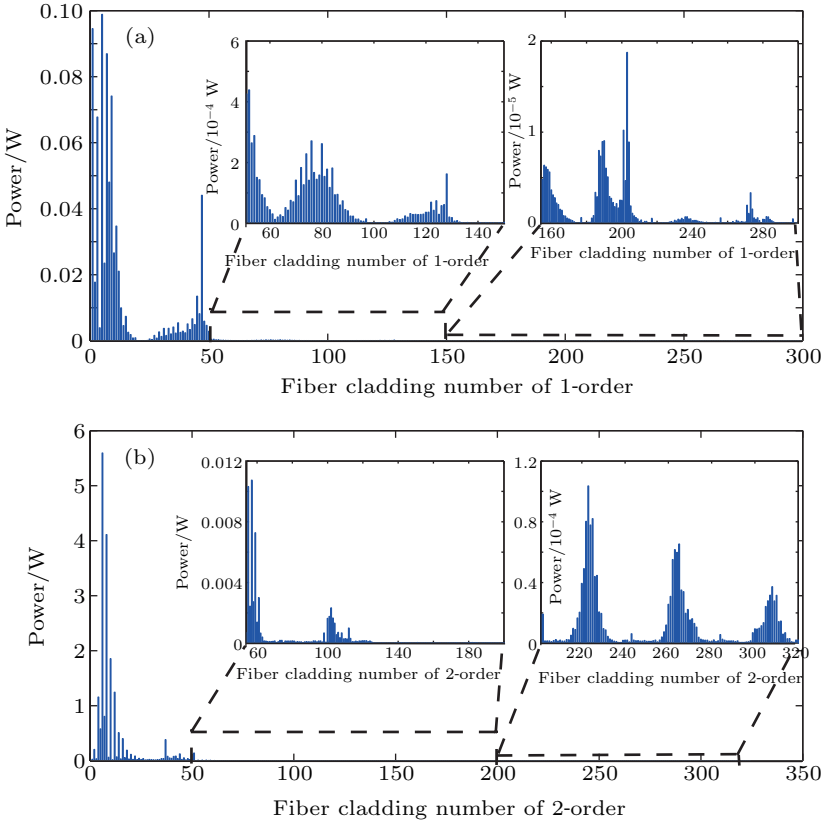


Fig. 7. (color online) (a) Gain spectrum (power) of the first-order cladding modes at the fiber end; (b) gain spectrum (power) of the second-order cladding modes at the fiber end.

Figure 8 shows the power distributions of the LP_{01} and the LP_{11} modes along the length of the fiber. The simulation results with and without mode coupling are indicated by the dashed line and the solid line, respectively. From Fig. 8, the mode-coupling power loss of the LP_{01} mode is close to 1 W (0.288%), and the power loss of the LP_{11} mode is 21.75 W (6.81%) with 750 W pump power launched into the gain fiber. The total signal ($\mathrm{LP}_{01}+\mathrm{LP}_{11}$) power loss is 22.73 W, with a proportion arriving at 3.4%, and the mode coupling loss occurs mainly in the coupling process of the LP_{11} mode into the second-order cladding modes.

Combined Fig. 5 and Fig. 8, some conclusions can be obtained. The mode coupling coefficient in the double clad fiber between core modes and clad modes decreases with rising ordinal number of clad modes. In another word, the bigger the ordinal number of the clad modes, the larger the difference between the field distributions of the clad mode and the core mode, resulting in a smaller mode coupling coefficient. The coupling coefficient of the LP_{11} mode with the clad modes is much bigger than that of the LP_{01} mode. This is mainly due to the much more similar effective refractive index of the LP_{11} mode with the clad mode, which in essence indicates a great similarity in the field distribution. Consequently, in the double clad fiber laser, the fundamental mode is the most stable mode because high order modes are easily submitted to all kinds of disturbance and transform into other modes, which is shown

in the simulation result in Fig. 8. When the fiber laser is influenced by external thermal disturbance, the propagation of the LP_{01} mode is relatively stable while the propagation of the LP_{11} mode suffers from large fluctuation caused by strong coupling effect.

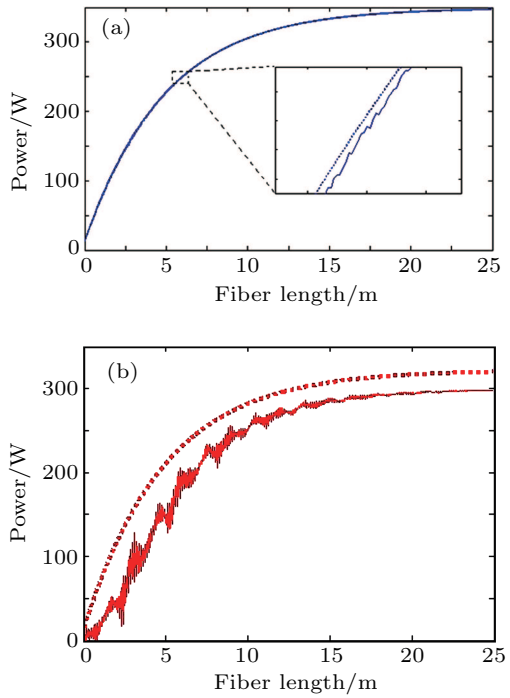


Fig. 8. (color online) (a) LP_{01} mode power without (dashed line) and with (solid line) thermal disturbance; (b) LP_{11} mode power without (dashed line) and with (solid line) thermal disturbance.

Using the coupled mode theory, we have described the interaction between the fiber core modes and the cladding modes, established a power attenuation model under thermally-induced refractive index variation conditions, and then obtained the fiber core loss under conventional cooling conditions[13] at multi-kW power levels.

5. Experimental setup and results

A double-clad ytterbium-doped fiber (YDF) laser amplifier was designed for thermally-induced core mode leakage measurement, and is depicted in Fig. 9. The fiber amplifier system parameters are listed in Table 1. A total of 42 fiber output laser diodes (LD), which each emit 25 W of pump power to provide a combined pumping power of 1 kW at 975 nm, were used as the pump source for launching into the active fiber. At the end of the amplifier, the laser output end cap was cleaved to an angle of 8°.

To verify the high-power fiber laser core mode leakage caused by the refractive index variations, this study separated the core mode power from the total fiber amplifier output power. A spectroscope that is highly reflective (HR) at 1080 nm and highly transmissive (HT) at 975 nm was placed at the output end of the amplifier to measure the pump components in the laser output and thus obtain both P_{pump} and $P_{\text{core}}+P_{\text{cladding}}$ (as shown in Fig. 9(a)). A cladding mode stripper (CMS) was then splice fused at the output end to remove both the cladding modes and the pump power from the output to obtain P_{core} (as shown in Fig. 9(b)).

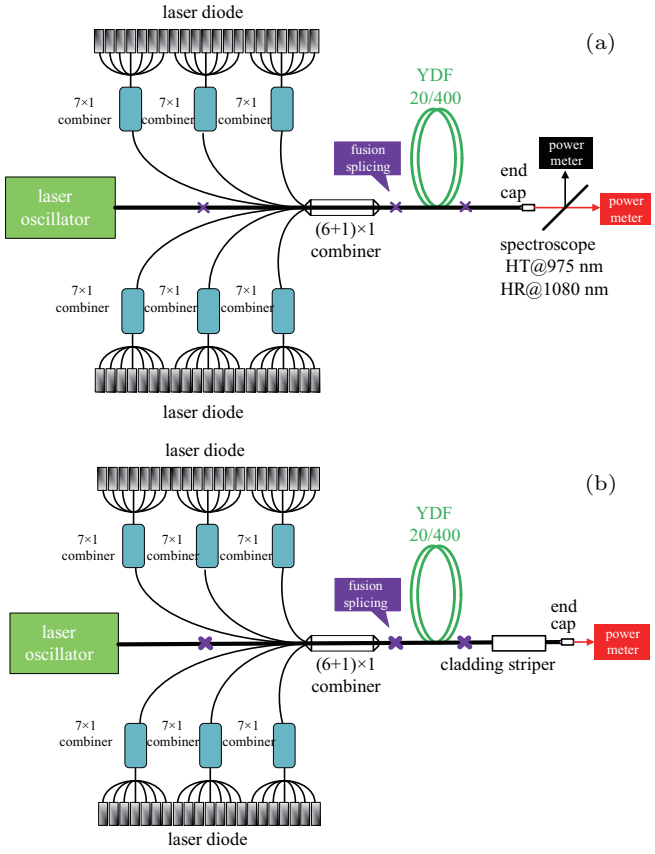


Fig. 9. (color online) Experimental setups without (a) and with (b) the cladding mode stripper for the fiber amplifier.

Figure 10(a) shows the output power ($P_{\text{core}}+P_{\text{cladding}}$, black curve), the remnant pump power (red curve), and the optical efficiency (P_{1080}/P_{975}, blue curve) with increasing pump power. When 750 W of pump power was launched into this fiber amplifier, 645 W (636 W in our simulation without the seed) of laser output power was obtained at 1080 nm, with a remnant pump power of 8.49 W@975 nm, an optical efficiency of 84.6%, and a beam quality of $M_x^2 = 1.59$ and $M_y^2 = 1.70$.

In the system shown in Fig. 9(b), following the removal of all pump power and cladding mode power by the CMS, the remaining pure fiber core mode output reached 562 W (without seed) for the core mode @1080 nm (black curve in Fig. 10(b)) when 750 W pump power was launched into the fiber amplifier. The corresponding core mode optical efficiency (blue curve in Fig. 10(b)) given by $P_{\text{core}}/P_{\text{pump}}$ was 70.2%.

As shown in Fig. 10(c), the proportion of the cladding mode was 13.1% with low gain, rising to 17.0% (blue curve) at a pump power of 750 W, and this suggests that the cladding mode increases by 3.9% with the increment in the pump power. The leakage of the core mode into the cladding that was caused by bending or fusion splices did not vary dramatically

with the increasing gain. Additionally, the fiber laser gain-guided phenomenon that occurred at multi-kilowatt levels appeared to be very weak and could thus be ignored. Therefore, the significant temperature variation that occurs with increasing pump power in the fiber amplifier system is the most likely reason for the leakage of the fiber core modes that is discussed in this paper.

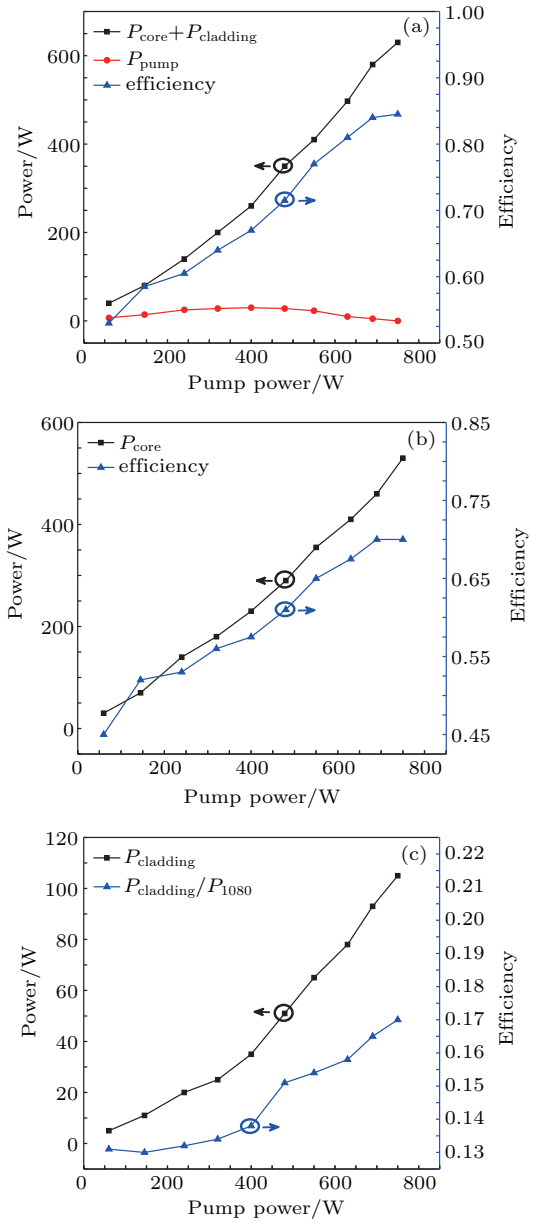


Fig. 10. (color online) Experimental results for (a) output power ($P_{core}+P_{cladding}$, black curve), remnant pump power (red curve), and optical efficiency ($P_{1080/P975}$, blue curve); (b) pure fiber core mode power (black curve) and corresponding core mode optical efficiency (blue curve); (c) cladding mode power (black curve) and corresponding cladding mode optical efficiency in fiber amplifier.

If a comparison is made between the simulation results (3.4%) and the experimental results (3.9%), the mode-coupling loss constitutes 87.1% of the total loss induced by the increasing pump power, which means that the leakage of the fiber core modes is the main part of the losses in multi-kilowatt fiber lasers.

6. Conclusion

This study develops a straightforward theoretical model to calculate the core mode losses in a fiber amplifier that demonstrates a specific level of cladding-mode coupling. The theory first provides a method to calculate the thermally-induced refractive index variation in the fiber laser. Then, a specific method is used to calculate the coupling coefficients and the coupling processes between the core and cladding modes. It is found that in a fiber laser, the thermally-induced refractive index variation is the main cause of the leakage of the fiber core modes. In a 750 W fiber laser, this leakage constitutes 3.4% of the total power.

This leakage process is irreversible and will lead to deterioration in both the laser efficiency and the power density. The analysis presented here indicates that the mode coupling loss of the fiber laser has a close relationship with the strength and the inhomogeneity of the thermal disturbance. Good heat dissipation and fiber temperature distribution compensation technology can significantly inhibit the mode coupling losses. Additionally, because a significant difference exists between the coupling strength of the fundamental mode and that of the higher order modes, improvement of the fiber laser beam quality through approaches such as mode selection techniques and mode filters can also prevent this kind of loss.

An experiment was also designed to measure the thermally-induced fiber amplifier mode leakage corresponding to the quantity in the calculations. There was 562 W core mode power in the total laser output power of 637 W at 1080 nm. The core mode leakage increased with increasing pump power. The experimentally measured results agreed well with the simulated results.

References

[1] Richardson D J, Nilsson J and Clarkson W A 2010 *J. Opt. Soc. B* **27** 63
[2] Jauregui C, Limpert J and Tünnermann A 2009 *Opt. Express* **17** 8476
[3] Hu M, Yang Y, Zheng Y, Liu G, Wang J, Liu K, Chen X, Zhao C, He B and Zhou J 2016 *Chin. Phys. Lett.* **33** 044208
[4] Huang C W, Chang C L, Jheng D Y, Hsu K Y, Huang S L and Huang D W 2012 *IEEE Photonics Journal* **4** 411
[5] Marcuse D 1976 *J. Opt. Soc.* **66** 216
[6] Gong M, Yuan Y, Li C, Yan P, Zhang H and Liao S 2007 *Opt. Express* **3236**
[7] Yin S, Yan P, Li C and Gong M 2008 *Chin. J. Lasers* **35** 835
[8] JaureguiC, Eidam T, OttoH, StutzkiF, JansenF, Limpert J and Tünnermann A 2012 *Opt. Express* **20** 441
[9] Erdogan T 1997 *J. Opt. Soc. A* **14** 1760
[10] Lee K S and Erdogan T 2000 *Appl. Opt.* **39** 1394
[11] Snyder A 1972 *J. Opt. Soc.* **62** 1267
[12] Yan P, Fu C, Xiao Q, Sun J, Li D, Zhang H and Gong M 2015 *Appl. Phys. B* **120** 623
[13] Fan Y, He B, Zhou J, Zheng J, Dai S, Zhao C, Wei Y and Lou Q 2012 *COL* **10** 111401